DAMAGE PREDICTION MODELS FOR REINFORCED CONCRETE BUILDINGS BASED ON NON-LINEAR ANALYSES WITH CONSIDERATION TO SOIL-STRUCTURE INTERACTION

Soshi Nakamura[1] ,Hiroshi Kawase[2] ,Naohiro Nakamura[3]

[1] *Researcher, R&D Institute, Takenaka Corporation, M. Eng.*
[2] *Professor, Disaster Prevention Research Institute, Kyoto University, Dr. Eng.*
[3] *Chief Researcher, R&D Institute, Takenaka Corporation, Dr. Eng.*
Email: nakamura.soushi@takenaka.co.jp, kawase@ zeisei.dpri.kyoto-u.ac.jp, nakamura.naohiro@takenaka.co.jp

ABSTRACT :

It is very important to construct analytical models that can express the actual seismic strength of buildings in order to estimate the damage to buildings for future earthquakes. Nagato and Kawase (2004) created such models by comparing building damage ratios based on the statistical damage survey for RC (reinforced concrete) buildings affected by the Hyogo-ken Nanbu earthquake and results from nonlinear response analyses of building models assumed under current building codes using simulated strong input motions. In this paper, Nagato's models are improved by considering both the effect of amplification of the earthquake motion in the surface sediments and the effect of the soil-structure interaction. As a result, more appropriate models are proposed, especially for 9 and 12 storied RC buildings.

KEYWORDS: damage evaluation, building, damage ratio, simulated strong motion, soil-structure interaction, the Hyogo-ken Nanbu earthquake

1. INTRODUCTION

In order to take measures to protect buildings against earthquake disasters in urban districts, it is very important to accurately estimate seismic motions caused by future earthquakes and then to quantitatively estimate the relationship between the seismic motions and the damage to buildings. For this purpose, appropriate damage prediction models which can evaluate the earthquake resistance performance of actual buildings are needed.

Nagato and Kawase (2004, hereafter referred to as the previous paper) made damage prediction models of buildings with resistance force profiles, which can simulate the observed damage ratio of buildings. They were calculated from the observed damage statistical data based on both the seismic response analyses results for the simulated strong motions of the Hyogo-ken Nanbu earthquake, which were estimated by Matsushima and Kawase (2000) and the statistical damage survey of buildings (hereafter referred to as prediction models).

However, soil-structure interaction was not taken into account for these prediction models. Furthermore, strong seismic motions calculated on the Osaka Group Formation, a soft diluvium layer with a shear wave velocity of 400m/s, were used as input waves acting on the foundation. Therefore, the amplification effects caused by the soft subsurface layer were not considered. In order to carry out more realistic evaluations, the models need to be improved with consideration to these effects.

In this study, first of all, subsurface layers in Nada and Higashi-Nada wards, which are subjected to our analyses, are modeled. Secondly, input motions acting on buildings under consideration of the amplification of subsurface layers are calculated by carrying out nonlinear soil response analyses. Thirdly, the dynamic soil stiffnesses of raft foundations and pile foundations are calculated based on the results from the equivalent-linear response analyses of the ground model. After that, seismic response analyses of buildings are carried out by applying these input motions and the dynamic soil stiffnesses to the prediction models as described in the previous paper. Finally, by comparing the results obtained from the analyses with the observed damage data, more realistic prediction models are constructed.

2.METHOD FOR CONSTRUCTING PREDICTION MODELS

In this study, damage prediction models for RC buildings are constructed. The investigation areas focused upon, where damage surveys of all RC buildings were made by the survey team (1996), are surrounded by the Hankyu-Kobe Line in Nada and Higashi-Nada Wards and R43 (Hanshin Highway R3)(See Fig.1). The prediction models are constructed basically using the method and assumptions based on the previous paper.

The differences in the method between this paper and the previous paper are as follows:

a) Input ground motions used for the response analyses are as amplified motions under the consideration of the effects of subsurface layers, but not a bedrock motion.

b) A sway model equipped with the dynamic soil stiffness is used as an analyses model.

Hereafter, the observed damage ratios obtained from the damage survey of all RC buildings are referred to as "ODRs", the calculated damage ratios by seismic response analyses are referred to as "CDRs", input ground motions calculated on the bedrock by Matsushima and Kawase are referred to as "bedrock motion", and input motions amplified by the effect of subsurface layers are referred to as "amplified motion" in this paper.

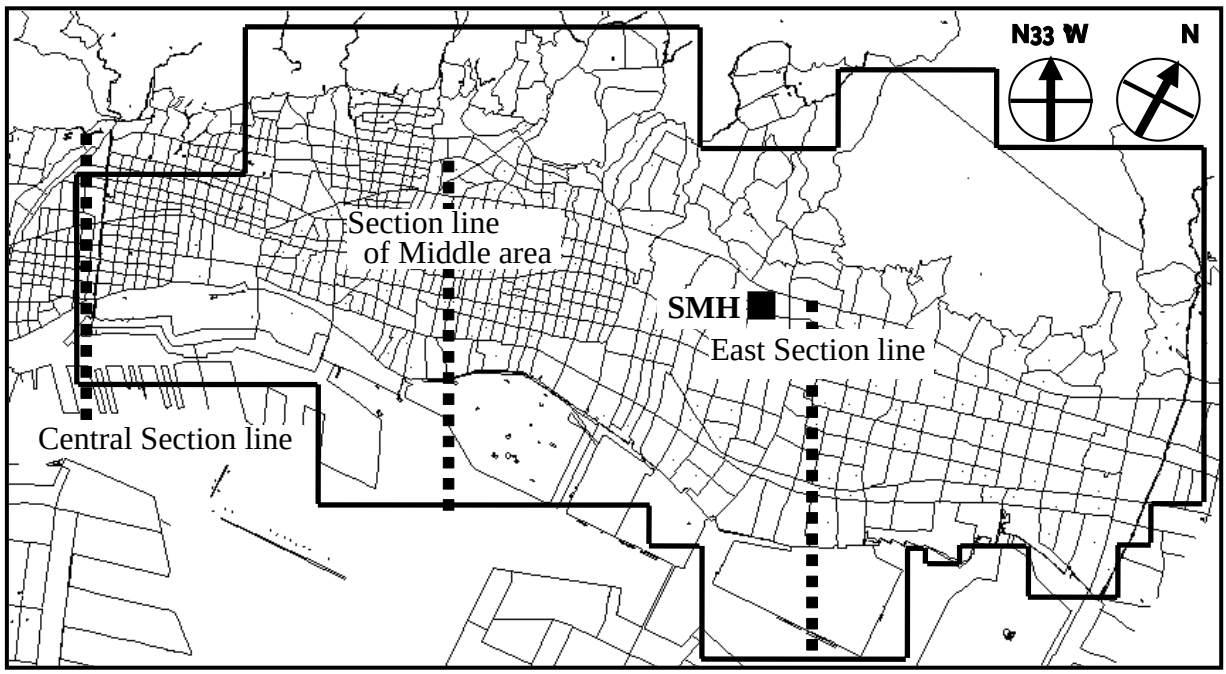

Fig.1 Analyzed area in Kobe and section lines used in this study

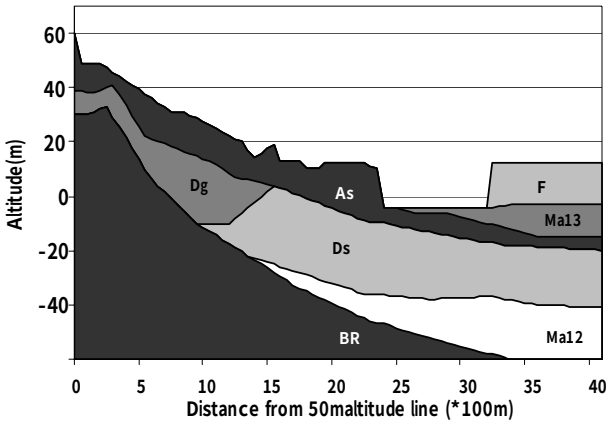

Fig.2 (a) Central section

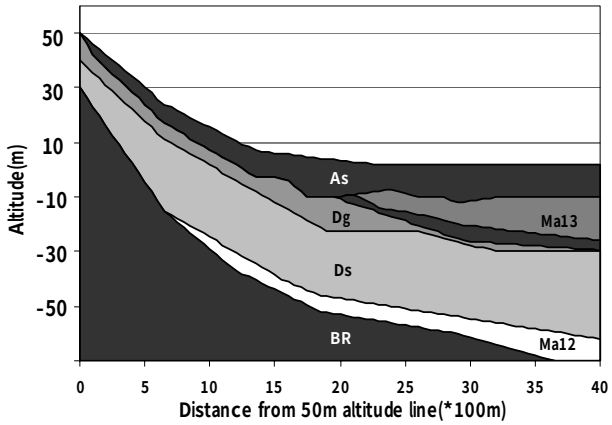

Fig.2 (b) East section

Fig.2 Central and East section of investigation areas

3. MODELING OF GROUND LAYER

3.1. Method for Modeling

Model of subsurface layers in the area subjected to investigations is set up as follows. First, the basic parameters for the section of subsurface layers are obtained using data from the East and the Central sections of Nada and Higashi-Nada Wards researched by Okimura (2004). Next, these sections are approximated using multi-polygonal lines for rational calculations. Fig.1 shows the positions of these sections. Fig.2 shows the approximated sections.

It is considered from 100 boring data obtained from the KOBE JIBANKUN (1999), which is the digital database software of underground information in Kobe such as the formation of layers and SPT (Standard Penetration Test) values linked to GIS, that in Nada ward alluviums are generally thin and diluviums appear on the surface in some places. Therefore, the surface layer (diluvium) in the middle of the East and Central section was set to be 1/2 of the East section in thickness.

Finally, from the three sections assumed above, models of subsurface layers in the entire target area were constructed using linear interpolation for the thickness of each layer.

3.2.Parameters and Non-linear Characteristics of Soil

Table.1 shows the parameters of each layer for the ground model based on the Okimura's research (2004). The non-linear characteristics of each layer are also set up based on the same research. However, with regard to an h- γ curve, when the value for strain approaches 0, that for damping also approaches 0. This is based on the highly accurate experiment results obtained in the literature written by Tatsuoka and Shibuya (1992). Fig.3 shows the h-γ and G- γ curves for Ma12 layer as example of the non-linear characteristics used in this paper.

Table.1 Soil parameter of subsurface layer

Layer			N value	Vs (m/s)	Density (tf/m^3)
Alluvium	Sand	As	23	219	1.8
Diluvium	Sand	Ds	44.9	336	1.95
	Gravel	Dg	51.9	356	2
Alluvium	Soil	Ma13	2.9	177	1.65
Diluvium	Soil	Ma12	4.4	267	1.7
Reclaimed	Reclaimed	F	11.3	192	1.85
Bedrock	Rock	BR	-	475	1.8

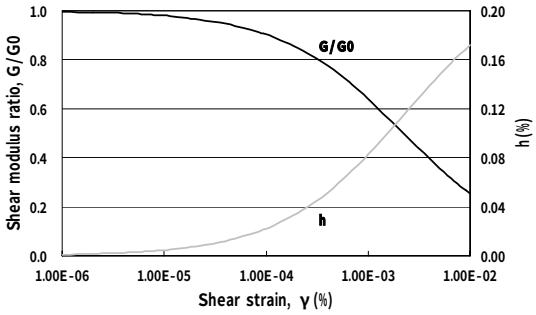

Fig.3 Dynamic deformation characteristics (ex.Ma12)

3.3 Ground Response Analyses

Response analyses of the ground are carried out using each parameter explained above. In the analyses, the equivalent linear analyses code DYNEQ by Yoshida and Suetomi (1996) based on the multiple reflection theory with consideration to the effects of plasticity of the soil is used.

Fig.4 shows the comparison of the maximum velocity distribution (N33°W components) between the bedrock motion and the amplified motion. It is clear that a distribution area where the maximum velocity of the amplified motion (Fig.4(a)) exceeds 90cm/s expands more widely than that of the bedrock motion (Fig.4(b)). This amplification effect is stronger where the predominant period is longer than 0.9sec.

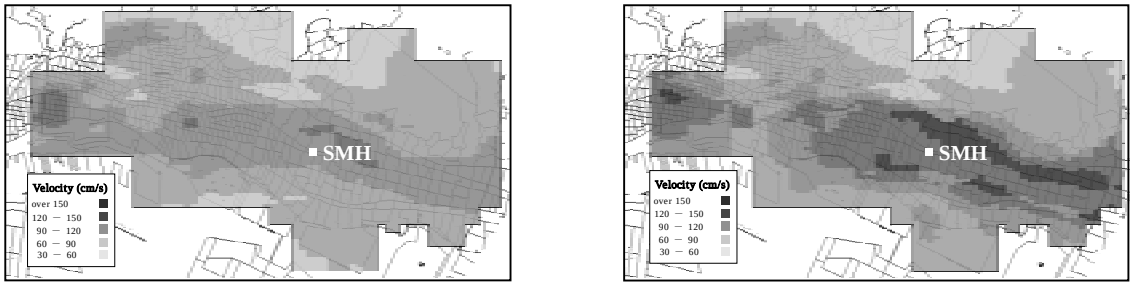

(a) Velocity of bedrock motion (b) Velocity of amplified motion

Fig.4 Distribution of maximum velocity

4. CALCULATION OF THE DYNAMIC SOIL STIFFNESS

4.1 Foundation Conditions of the Buildings

The following conditions are set up for four types of building models used for the investigations (hereafter referred to as 3F, 6F, 9F and 12F models). The plane shape of each model is designed according to the previous paper. Fig.5 (a) shows the plane shape of the 3F model. Fig.5 (b) shows those of the 6F~12F models.

For all models, directions along the longitudinal direction of the models are subjected to investigations. Because the response values increase.

The types of foundations are established as follows with reference to the results of research into the damage to building foundations affected by the Hyogo-ken Nanbu earthquake (1998).

1) 3F model: A raft foundation is considered.
2) 6~12 F models: Raft foundations are considered for areas where bedrock outcrops and pile foundations are considered for the other areas. The pile conditions are set up as follows in the light of data (in 25 cases) with respect to cast-in-place piles for RC and SRC structures in Higashi-Nada and Nada wards, which are described in the literature (1998).
   a) Pile arrangement: 24 piles for each model are placed under every column of 1st floor.
   b) Diameter of pile: 1.6m for the 6F model, 1.8m for the 9F model and 2.0m for the 12F model are set.
   c) Bottom of pile: Piles are embedded to a depth of 1.0m for diluviums (Dg, Ds) through reclaimed ground or alluviums.

4.2 Method for Calculating The Dynamic Soil Stiffness

In this study, sway components of the dynamic soil stiffness are estimated and rocking components are set to be rigid for the following reason. With respect to the low storied model (3F model) with a raft foundation, the effects of rocking are thought to be slight. Due to the fact that the length of the pile used for the pile foundation which is considered for the 6F~12F models is short as a whole, it is considered that the vertical stiffness is larger than the horizontal stiffness and that the effects of the rocking component are small.

Methods for calculating the dynamic soil stiffness are based on the relatively simple method shown in the literature written by Sako (2006), which is proposed for practical design. This is because there are great deals of cases (3219 points*4 types of buildings) subjected to analyses. The validity of these methods is confirmed by comparing them with the theoretical solution and the precise method.

1) Raft Foundation
   In an area where the bedrock forms outcrops, the stiffness is calculated using the practical expression by Wolf (1994) for the static ground stiffness along the long side of the rectangular rigid foundation on a uniform halfspace. The damping of ground is calculated as an equivalent viscous boundary damper for the foundation area.

2) Pile Foundation
   The following methods are used for the pile foundation according to Sako (2006) in which details can be seen.
   a) The coefficient of the pile group for the dynamic soil stiffness is calculated
   b) The constant of the spring around piles and the damping coefficient are estimated for each layer of the bedrock using the Francis's formula (1964) and the Gazetas's formula (1984).
   c) The constant of the dynamic soil stiffness is estimated from the entire pile group at its highest position using the theoretical solution with respect to elastic bearing beams.
   d) The damping ratio of the dynamic soil stiffness of the pile group foundation is estimated based on the Sako's method (2006) by considering the effects of material damping of the soil in the natural frequency range or less as well as the effects of radiation damping in a range higher than that. In the latter case, the frequency used to obtain the damping ratio is the coupled system natural frequency.

5. SEISMIC RESPONSE ANALYSES

5.1 Analyses Model

The damage prediction model is constructed based on the results of seismic response analyses of building models to which amplified motions are input. The response analyses models are multi-degree-freedom models made with consideration to the dynamic soil stiffness. The restoring force characteristics of each level are of the so-called Degrading-Trilinear hysteresis type. The instantaneous stiffness proportioned damping is used (damping ratio h=5%). The weight of each level and the skeleton curve are set up under the same conditions as those explained in the previous paper. The analyses are carried out using the Newmark's β method with β = 1/4 and time interval Δt=0.005sec.

Fig.6 (a) shows the concept view of the analyses model. The amplified motion calculated in chapter 3 is input to a model with the dynamic soil stiffness fitted to the lower end of the building foundations, which were set in chapter 4 (hereafter referred to as a sway model). At the same time, analyses in which the amplified motion is input to a model without any soil stiffness (hereafter referred to as a base-fixed model) are carried out for comparison. The distribution of the strength is calculated using the probability density function for RC structures estimated by Shibata (1980) in the same manner as that described in the previous paper. To make calculation simple, the strength distribution was divided into the 12 parts (See Fig.6 (b)).

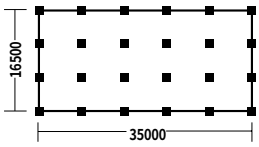

(a) 3 storied model

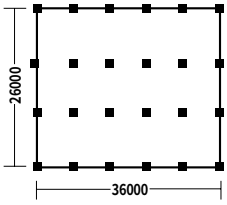

(b) 6~12 storied model

Fig.5 Plane plan of building model

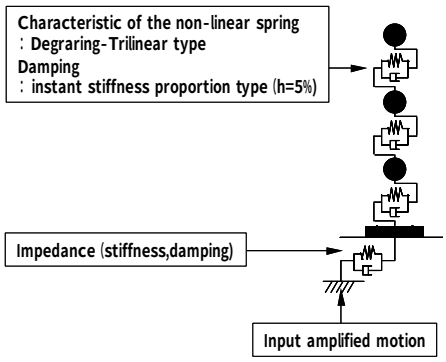

(a) concept view

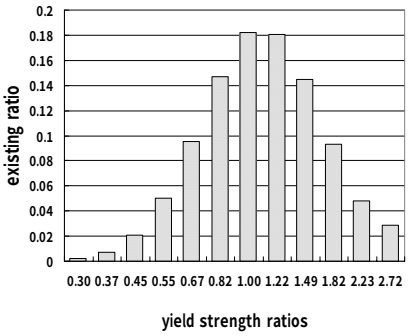

(b) yield strength

Fig.6 Concept view and distribution of yield strength

5.2 Response Characteristics

First, the effects of the addition of the dynamic soil stiffness upon responses are analyzed. Fig.7 shows the mean value of the maximum story drift angles at 3219 points for the 9F base-fixed model and sway model. This is the result of the model whose yield strength ratio is the median value (1.0). The amplified motion is input to both models and α identified in the previous paper is used. In this figure "old" means those constructed before 1981 and "new" means after 1981, when significant building code modifications were made. The response value of the sway model becomes slightly smaller than that of the base-fixed models, especially in the lower part of the buildings. It is thought that this is due to the effects of interaction of the dynamic soil stiffness.

Next, the maximum story drift angle of both models in Sumiyoshi-Honmachi where the maximum velocity was observed as mentioned above is shown in Fig.8. The response of sway model is not always smaller than base-fixed models, especially in the middle part of the buildings. This is because the base-fixed models show the strong nonlinear behavior in the lower part of the building, which absorb most of the input energy. It is considered that the effects of soil-structure interaction are canceled to some extent, due to the shift of the natural period caused by the addition of the dynamic soil stiffness. This tendency was most conspicuously seen in the 9F model. But similar tendency was also seen in the other models.

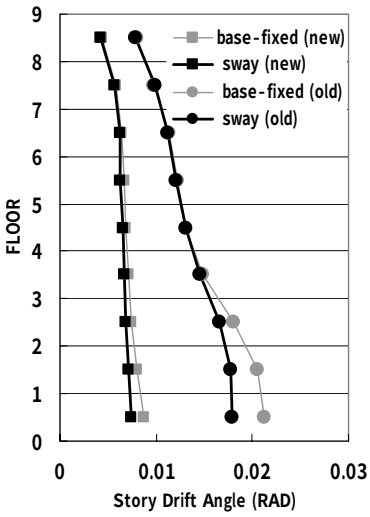

Fig.7 Maximum story drift angle (mean value of all of point)

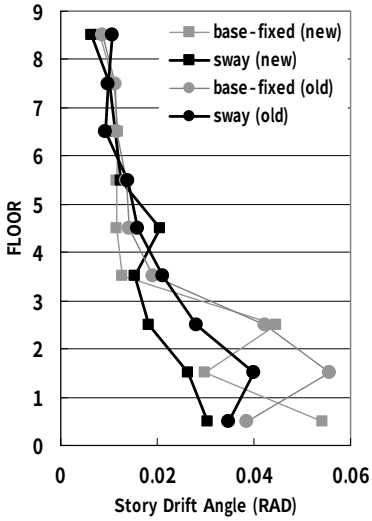

Fig.8 Maximum story drift angle (at point SMH)

5.3 Calculation of CDRs and Fitting of Strength Ratio α

Fig.9 compares the CDRs of the sway model and the base-fixed model in the case of the strength ratio α (hereafter referred to as α) obtained in the previous paper. By using this α, CDRs in the previous paper match ODRs. The amplified motion is used as an input motion to the sway model and the base-fixed model. The meaning of "old model" and "new model" is the same as Fig.7 and 8. The CDRs described in the previous paper is a result obtained by inputting the bedrock motion to the base-fixed model.

It should be noted that the difference in the damage ratios between the model in the previous paper and the base-fixed model is caused by the amplification effect in the subsurface layer. The difference between the base-fixed model and the sway model is caused by the effects of soil-structure interaction. This figure indicates that the amplification effect in the subsurface layer and the soil-structure interaction effect for both the 3F and 6F models nearly cancel each other so that CDRs calculated with the previous α nearly agree with ODRs for both cases.

On the other hand, CDRs of the 9F and 12F base-fixed models are much higher than their ODRs because both models are greatly affected by the amplification caused by the subsurface layer. As a result, in order to match CDRs with ODRs, the strength ratio α needs to be increased from the previous value.

Following the procedure of the previous paper, response analyses were repeated until CDRs agreed with ODRs by changing the value for α by 0.05 at each time.

Fig.10 shows the values for the α when CDRs agree with ODRs. The previous α is also shown in the same figure. As mentioned above, it was not necessary to greatly change the strength ratios for the 3F and 6F models from the previous α. However, as for the 9F and 12F models, the new α was increased by about 0.5 from the previous α.

5.4 Comparison in Damage Ratio Distribution

Figs.11 shows the distributions of the damage ratios of ODRs and CDRs for the 9F old (constructed before 1981) buildings using a sway model. It can be said from the comparison of these distributions that the distribution of districts having serious damage with a damage ratio exceeding 0.2 is fairly well simulated. However, with respect to the distribution of areas with a damage ratio less than 0.1, those for CDRs are more widely distributed than those for ODRs. It is considered that this is because small damage ratios do not appear in ODRs due to the limited number of buildings in each small area. For example, 10 or more buildings are needed in order to have a damage ratio less than 0.1. This tendency is seen quite clearly in the 9F and 12F models.

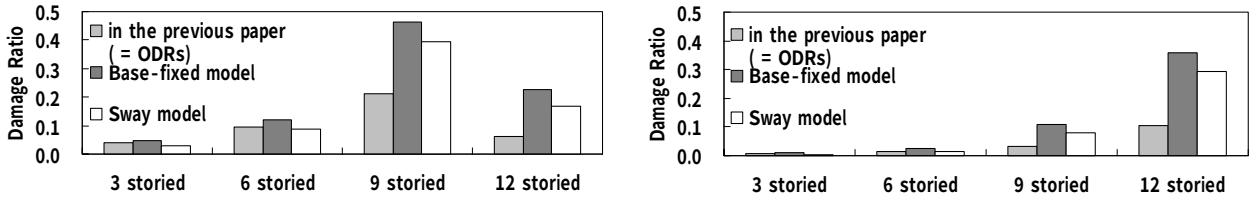

(a) old model (b) new model

Fig.9 Damage ratios of each model

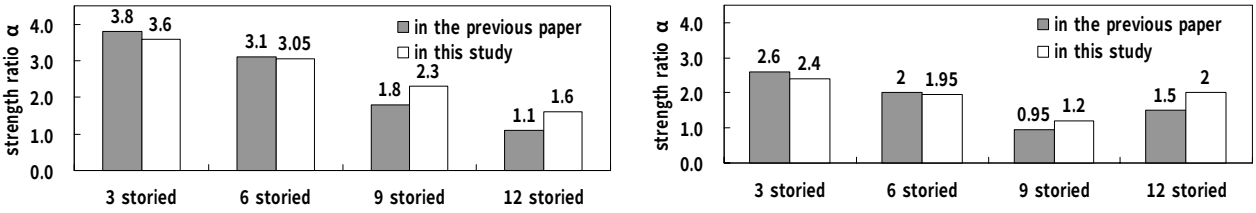

(a) old model (b) new model

Fig.10 Estimated strength ratio α of each model

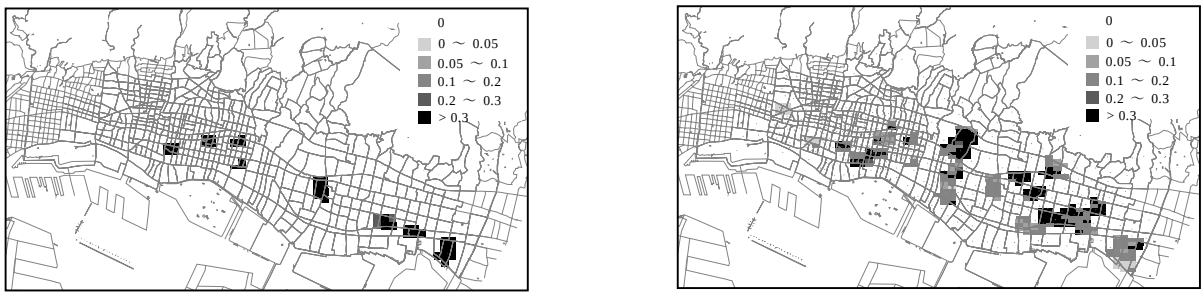

(a) observed damage ratios (b) calculated damage ratios

Fig.11 Distribution of damage ratios (9F old model)

6. CONCLUSIONS

In this study, the dynamic soil stiffness were introduced into numerical analyses models for damage prediction constructed by Nagato and Kawase (2004), together with the amplification in the subsurface layers in Nada and Higashi-Nada Wards, for the purpose of improving the accuracy of the models. The results obtained from this study are summarized as follows:

1) Due to the amplification generated by the effects of the subsurface layers in Nada and Higashi-Nada Wards, the peak ground velocities of the simulated strong motion were increased. Areas where predominant periods are longer than 0.9sec are greatly affected by this tendency.
2) In the 3F and 6F models, the amplification effect caused by the subsurface layer and the effect of soil-structure interaction canceled out each other. However, in the 9F and 12F models the amplification effect greatly exceeded the soil-structure interaction effect. Thus there was a need to increase the relative strength of the buildings from those obtained in the previous paper. It is thought that this is because the components of long period of the ground motion were amplified as mentioned in 1), while the effects of soil-structure interaction for long period buildings are not so much.
3) The distribution of CDRs by the newly identified strength ratio was compared with ODRs. The distribution of ratios for serious damage was able to be simulated fairly well. The difference between the results of this study and those in the previous paper was comparatively small. It is considered from

this fact that the distribution of strong ground motions on the engineering bedrock, created by the edge-effects (Matsushima and Kawase, 2000), played a major role upon the spatial distribution of the damage ratios observed in Kobe during the Hyogo-ken Nanbu earthquake of 1995.

REFERENCES

Nagato, K. and Kawase, H. (2004). Damage evaluation models of reinforced concrete buildings based on the damage statistics and simulated strong motions during the 1995 Hyogo-ken Nanbu earthquake. *Earthqukake Engineering And Structural Dynamics*, **Vol.33**, 755-774

Matsuhima, S and Kawase, H. (2000). Multiple asperity source model of the Hyogo-ken Nanbu earthquake of 1995 and strong motion simulation in Kobe. *Journal of Structural and Construction Engineering*, **No.534**, 33-40 (in Japanese)

Reinforced Concrete Structure Research Committee (1996). Report on damage statistics for reinforced concrete buildings during the Hyogo-ken Nanbu earthquake. Kinki Branch, Architectural Institute of Japan (in Japanese)

Shibata, A. (1980). Prediction of the probability of earthquake damage to reinforced concrete building groups in a city. *Proceedings of the 7th World Conference on Earthquake Engineering*, **Vol.4**, 395-402

Okimura, T. (2004). The Report of the Great Hanshin-Awaji Earthquake Memorial Research Institute, **Vol.10**, 5-22 (in Japanese)

City Government of Kobe (1999). KOBE JIBANKUN, User's manual (in Japanese)

Tatsuoka, F. and Shibuya, S. (1991). Deformation characteristics of soils and rocks from field and laboratory tests, *Proc. of the 9th Asian Regional Conf. on SMFE*, **Vol.2**, 101-170

Yoshida, N. and Suetomi, I. (1996). DYNEQ: A computer program for dynamic analysis of level ground based on equivalent linear method, *Reports of Engineering Research Institute, Sato Kogyo Co.Ltd.* , 61-70

Editorial Committee for the Report on the Hanshin-Awaji Earthquake Disaster (1998). Report on the Hanshin-Awaji earthquake disaster-wooden structure and damage to building foundations-, Architectural Institute of Japan, **Vol.4**, 281-293 (in Japanese)

Sako, Y. (2006). Chapter 6 in Seismic response analysis and design of buildings considering dynamic soil-structure interaction, Architectural Institute of Japan, 152-167 (in Japanese)

Wolf, J.P. (1994). Chapter 2, Foundation on surface of homogenous soil halfspace in Foundation vibration analysis using simple physical models, PTR Prentice Hall, 33-34

Francis, A.J. (1964). Analysis of pile groups with flexural resistance, *J. Soil Mech. and Foundations Div., ASCE*, **Vol.90:No.sm3**, 1-32

Gazetas, G. and Dobry, R. (1984). Horizontal response of piles in layered soils, *J Geotech. Engrg. Div., ASCE*, **Vol.110**, 20-40

Yoshida, K. (2006). Chapter 5 in Seismic response analysis and design of buildings considering dynamic soil-structure interaction, Architectural Institute of Japan, 127-131 (in Japanese)